The Journal of Experimental Biology 209, 599-609
Published by The Company of Biologists 2006
doi:10.1242/jeb.02059

Microtubule-dependent relocation of branchial V-H$^+$-ATPase to the basolateral membrane in the Pacific spiny dogfish (*Squalus acanthias*): a role in base secretion

Martin Tresguerres*, Scott K. Parks, Fumi Katoh and Greg G. Goss

Dept of Biological Sciences, University of Alberta, Edmonton, Alberta, T5G 2E9, Canada and Bamfield Marine Research Centre, Bamfield, British Columbia, V0R 1B0, Canada

*Author for correspondence (e-mail: martint@ualberta.ca)

Accepted 22 December 2005

Summary

We have previously shown that continuous intravenous infusion of $NaHCO_3$ for 24 h (~1000 μmol kg^{-1} h^{-1}) results in the relocation of V-H$^+$-ATPase from the cytoplasm to the basolateral membrane in the gills of the Pacific dogfish. To further investigate this putative base-secretive process we performed similar experiments with the addition of colchicine, an inhibitor of cytoskeleton-dependent cellular trafficking processes. Blood pH and plasma total CO_2 were significantly higher in the colchicines-treated, HCO_3^--infused fish compared with fish infused with HCO_3^- alone. The effect of colchicine was highest after 24 h of infusion (8.33±0.06 *vs* 8.02±0.03 pH units, 15.72±3.29 *vs* 6.74±1.34 mmol CO_2 l^{-1}, *N*=5). Immunohistochemistry and western blotting confirmed that colchicine blocked the transit of V-H$^+$-ATPase to the basolateral membrane. Furthermore, western blotting analyses from whole gill and cell membrane samples suggest that the short-term (6 h) response to alkaline stress consists of relocation of V-H$^+$-ATPases already present in the cell to the basolateral membrane, while in the longer term (24 h) there is both relocation of pre-existent enzyme and upregulation in the synthesis of new units. Our results strongly suggest that cellular relocation of V-H$^+$-ATPase is necessary for enhanced HCO_3^- secretion across the gills of the Pacific dogfish.

Key words: fish, dogfish, *Squalus acanthias*, gill, acid base regulation, H$^+$-ATPase, base infusion, alkalosis, colchicine, basolateral H$^+$-ATPase, microtubule, vesicular trafficking.

Introduction

The gills of marine elasmobranchs account for over 97% of the acid/base relevant ion fluxes between the animal and the environment (Heisler, 1988). Recently, distinct Na$^+$/K$^+$-ATPase- and H$^+$-ATPase-rich cells have been described in the gill epithelia of seawater and seawater-acclimated Atlantic stingrays (*Dasyatis sabina*) (Piermarini and Evans, 2001) and the Pacific spiny dogfish (*Squalus acanthias*) (Tresguerres et al., 2005). Based on analogies to the mammalian kidney, Na$^+$/K$^+$-ATPase-rich cells were proposed to be involved in net acid secretion, while H$^+$-ATPase-rich cells were thought to participate in net base secretion (Piermarini and Evans, 2001). The proposed model for base secretion predicts that CO_2 from the blood diffuses into the cell, where it is hydrated into H$^+$ and HCO_3^- by the enzyme carbonic anhydrase (CA). HCO_3^- leaves the cell across the apical membrane in exchange for Cl$^-$ from the water through an anion exchanger. The H$^+$ is then pumped back to the blood by the V-H$^+$-ATPase (H$^+$-ATPase). The coordinated action of these proteins would result in net base secretion (reviewed by Evans et al., 2005). Immunodetection of a Pendrin-like protein, a putative Cl$^-$/HCO_3^- exchanger, in the apical membrane of the H$^+$-ATPase-rich cells of the Atlantic stingray provided the first conclusive evidence for the involvement of these cells in base secretion (Piermarini et al., 2002). More recently, Pendrin immunoreactivity was also detected in the apical membrane of gill cells of *S. acanthias* (Evans et al., 2004), suggesting that the model may be more widespread among marine elasmobranches.

However, as explained above, the model for base secretion requires the H$^+$-ATPase to be located in the basolateral membrane, yet the previous studies on marine elasmobranches demonstrated a distinct cytoplasmic staining pattern (Piermarini and Evans, 2001; Piermarini et al., 2002; Wilson et al., 1997). Although it was suggested that H$^+$-ATPase would be recycled between a cytoplasmic pool of vesicles and the basolateral membrane (Piermarini and Evans, 2001), definitive evidence was lacking. In our previous paper (Tresguerres et al., 2005), we demonstrated that induction of blood alkalosis by intravenous infusion of $NaHCO_3$ for 24 h produces a dramatic cellular remodelling in the H$^+$-ATPase-rich cells involving a switch in the H$^+$-ATPase localization

from primarily cytoplasmic to distinctly basolateral. Our results support the hypotheses that the H^+-ATPase-rich cells mediate net base secretion and suggest that trafficking of H^+-ATPase between the cytoplasm and the basolateral membrane indeed exists and it is especially active during blood alkalosis. The current study was designed to investigate whether the cytoskeleton-mediated movement of H^+-ATPase from the cytoplasm to the basolateral membrane under alkaline stress is necessary for increased capacity for base secretion. To address this possibility, we repeated our base-infusion protocol (Tresguerres et al., 2005) with the addition of colchicine, a plant alkaloid extract that disrupts microtubule assembly and inhibits processes that require an intact cytoskeleton for the relocation of proteins within the cell (Brown, 2000; Stephens and Edds, 1976).

Materials and methods

Animals

Pacific spiny dogfish (*Squalus acanthias* L.) from the Trevor Channel, Vancouver Island, BC, Canada were caught by hook and bait and transferred immediately to the Bamfield Marine Research Centre. Dogfish were held in a 288 m^3 tank provided with flowing seawater (11°C, 31‰ salinity). The 6 h- and 24 h-infusion experiments were conducted in June and September 2005, respectively. Fish were fed once a week with flounder and squid while being housed in this tank, except for at least one day previous to the experiment.

Antibodies and reagents

Rabbit anti-H^+-ATPase was raised against a synthetic peptide based on the highly conserved and hydrophilic region in the A-subunit (Katoh et al., 2003). This antibody has been successfully used in gills of various fish species, including dogfish (Tresguerres et al., 2005). A donkey anti-rabbit fluorescent secondary antibody (Li-Cor, Inc., Lincoln, NE, USA) was used for western analysis. Unless otherwise mentioned, the reagents used in this study were purchased from Sigma (St Louis, MO, USA).

Surgery and acid–base infusions

A total of 27 animals (mean body mass, 2.31±0.14 kg) were removed from the housing tank and cannulated for this study. Fish were caught by hand, anesthetized with 1:10 000 tricaine methanesulfonate (TMS; AquaLife, Syndel Laboratories Ltd, Vancouver, BC, Canada) and transferred to an operating table, where the gills were irrigated with aerated seawater containing TMS. Two cannulae (PE-50; Clay-Adams, Persippany, NJ, USA) were fitted into the caudal vein and artery. The incision was sutured with stitches and a small volume of a heparanized (50 i.u. ml^{-1} Na^+-heparin) 500 mmol l^{-1} NaCl solution was injected before blocking the tubing by tying up the end. The animals were transferred to experimental boxes (36 litre) with aerated flowing seawater. After a 24 h recovery period, the venous cannula was connected to a Gilson minipuls peristaltic pump (Middleton, WI, USA), and the experimental solution was infused at a rate of 4.47±0.22 ml h^{-1} kg^{-1}. The arterial cannula was used to withdraw blood samples during the course of the experiment.

Table 1. *Base and NaCl infusion rates in each of the infusion treatments*

	Infusion	[HCO_3^-]	[Na^+]	[Cl^-]
6 h (*N*=4)	Col-NaCl	–	2546±501	2546±501
	BIF	964±63	1928±107	964±63
	Col-BIF	1055±69	2111±139	1055±69
24 h (*N*=5)	Col-NaCl	–	2415±417	2415±417
	BIF	1081±108	2162±216	1081±108
	Col-BIF	1152±124	2304±248	1152±124

Values are means ± s.e.m. and are expressed as μequiv. kg^{-1} h^{-1}.

In order to induce alkalosis in the blood, fish were infused with 250 mmol l^{-1} $NaHCO_3$ to achieve a nominal HCO_3 infusion rate of 1000 μmol kg^{-1} h^{-1} (base-infused fish, BIF). To minimize osmotic disturbances, the osmolarity of the infusion solutions was adjusted to 1000 mosmol l^{-1} with the addition of NaCl. Animals infused with 500 mmol l^{-1} NaCl and treated with colchicine (col-NaCl IF) served as an additional control. Table 1 shows the HCO_3^- and NaCl loads in the 6 h and 24 h infusions.

Blood samples and analytical procedures on plasma samples

Arterial blood samples (400 μl) were taken at time 0 and subsequently every 1 h in the 6 h infusions (*N*=4) and at times 0, 1, 3, 6, 9, 12, 18 and 24 h in the 24 h-infusion experiments (*N*=5). After the blood extraction, an equal volume of heparanized 500 mmol l^{-1} NaCl saline was injected into the fish to minimize changes in blood volume and prevent clotting. A ~50 μl blood sample was used for haematocrit analysis. Blood pH was measured using calibrated electrodes [Radiometer G299A (Copenhagen, Denmark) or Accumet micro-size pH electrode model 13-620-94 (Fisher Scientific, Pittsburgh, PA, USA)]. Blood samples were centrifuged at 12 000 ***g*** to obtain plasma. Plasma total CO_2 (TCO_2) was measured immediately in samples from the 6 h infusions, while samples from the 24 h experiments were frozen and shipped in a dry-shipper to Dr Colin Brauner's lab at the University of British Columbia, Vancouver, BC, Canada. TCO_2 was analyzed using a Corning 965 carbon dioxide analyzer (Ciba Corning Diagnostic, Halstead, Essex, UK). A plasma sample was preserved at –80°C for later analysis of osmolarity (Precision Systems Inc., Natick, MA, USA), Na^+ concentration (atomic absorption spectrophotometer; model 3300; Perkin-Elmer, Norwalk, CT, USA) and Cl^- concentration (Zall et al., 1956).

Colchicine treatment

A fresh colchicine stock solution (10 mg ml^{-1}) in 500 mmol l^{-1} NaCl was made just before each injection time. Colchicine-treated fish were injected with a bolus dose of 15 mg kg^{-1} of colchicine at *t*=0. A nominal concentration of

10^{-4} mmol l^{-1} (cf. Maetz and Pic, 1976) in the plasma was targeted. However, colchicine has a half-life in plasma of ~1 h (Moffat, 1986) and therefore we followed the protocol by Gilmour et al. (1998) and injected half the initial dose every 6 h (at t=6, 12, 18 h). This protocol was applied to the colchicine-treated, base-infused fish (col-BIF) and col-NaCl infused fish. Fish infused with base alone were injected with an equivalent volume of 500 mmol l^{-1} NaCl at the same experimental times.

Terminal sampling

After the blood sample at either 6 or 24 h of infusion, fish were killed by injection of 5 ml of a saturated KCl solution. Gill samples were immediately excised and either snap frozen in liquid nitrogen for later western blot analyses or placed in fixative (see below) for immunohistochemistry.

Immunohistochemistry

Gill samples for immunohistochemistry were fixed in 3% paraformaldehyde, 0.1 mmol l^{-1} cacodylate buffer (pH 7.4) for 6 h at 4°C and processed for immunohistochemistry as described in Tresguerres et al. (2005). Three consecutive gill filaments were embedded together into paraffin blocks and sectioned every 4 μm. Sections from each block from the trailing edge of the filaments were immunostained and analyzed. After deparaffination in toluene, hydration in a decreasing ethanol series and double distilled water (ddH_2O), sections were blocked with 2% normal goat serum (NGS) for 30 min and incubated overnight at 4°C with the anti H^+-ATPase antibody, which was diluted 1:1000 in 2% NGS, 0.1% bovine serum albumin, 0.02% keyhole limpet haemocyanin, 0.01% NaN_3 in 10 mmol l^{-1} phosphate-buffered saline, pH 7.4. The next steps were performed using the Vectastain ABC kit (Vector Laboratories, Burlingame, CA, USA), following the manufacturer's directions. Some sections were stained using a goat anti-rabbit antibody bound to 5 nm gold particles (BBInternational, Llanislen, Cardiff, UK) for 60 min, followed by the silver enhancement method (10 min, BBInternational), and a 30-s incubation in Harris's hematoxylin (Humason, 1962) to stain nuclei. Since we found no qualitative differences, results from both methods were combined. Gill sections incubated without the primary antibody never showed specific staining, regardless of the staining method used.

To detect potential changes in the number of H^+-ATPase-rich cells in the different treatments, we counted the number of labelled cells per intralamellar space (# cells/IL). This was done by analyzing micrographs taken at a magnification of 400× from randomly selected ILs from at least two gill filaments per fish. The total number of ILs analyzed was 40 in the 6 h-infusion experiments and 50 in the 24 h infusions. The cellular distribution analysis was performed on 2000× micrographs from around 200 cells per treatment.

Western blot analysis

Frozen gill samples were weighed, immersed in liquid nitrogen and pulverized in a porcelain grinder. The resultant powder was resuspended in 1:10 w/v of ice-cold homogenization buffer [250 mmol l^{-1} sucrose, 1 mmol l^{-1} EDTA, 30 mmol l^{-1} Tris, 100 mg ml^{-1} PMSF (phenyl methyl sulphonyl fluoride) and 2 mg ml^{-1} pepstatin, pH 7.4] and sonicated on ice for 20 s. Debris was removed by low-speed centrifugation (3000 ***g*** for 10 min, 4°C), and a sample of the supernatant (whole gill homogenate) was stored at –80°C. The rest of the sample was then subjected to a medium speed centrifugation (20 800 ***g*** for 60 min, 4°C), and the pellet was resuspended in homogenization buffer and stored at –80°C as the plasma membrane fraction. This fraction contains almost all of the Na^+/K^+-ATPase activity as a marker of the basolateral membrane. However, it is unlikely that much of the microsomal fraction is pelleted in this medium-speed fraction, because microsomal vesicles are typically not pelleted until much higher forces (~1 000 000 ***g***) are encountered. Samples of both the whole gill and gill membrane fractions were saved for protein determination analysis (Pierce, Rockford, IL, USA), which was performed in triplicate. On the day of the western analysis, processed gill samples were thawed and combined with 2× Laemmli buffer (Laemmli, 1970). 15 μg of total protein were separated in a 7.5% polyacrylamide mini-gel (45 min at 180 V) and transferred to a nitrocellulose (NC) membrane (1 h at 100 V) using a wet transfer cell (Bio-Rad Laboratories, Inc., Hercules, CA, USA). Following blocking [5% chicken ovalbumin in 0.5 mol l^{-1} Tris-buffered saline (TBS) with 0.1% Triton-X, pH 8.0, overnight at 4°C], the NC membranes were incubated with the primary antibody against the A-subunit of the H^+-ATPase with gentle agitation at 4°C overnight. After four washes of 15 min each with TBS-Triton X (0.2%), the NC membrane was blocked for 15 min and then incubated with the fluorescent secondary antibody at room temperature for 2 h. Bands were visualized and quantified using the Odyssey infrared imaging system and software (Li-Cor, Inc.). Differences in loading were corrected by quantifying the total protein concentration in each lane after staining with Coomassie Brilliant Blue. The gill membrane sample from one NaCl-infused, colchicine-treated fish was loaded in every gel and it was used to standardize samples from different gels. Values are given as arbitrary fluorometric units (a.f.u.). NC membranes incubated with blocking buffer without the primary antibody served as controls and did not show any labelling.

Statistics

All data are given as means ± s.e.m. Differences between groups were tested using one-way analysis of variance (1-way ANOVA) or repeated-measures analysis of variance (RM-ANOVA) when appropriate. When RM-ANOVA was used, differences at each sampling time were tested using 1-way ANOVA. For analysis of blood pH and TCO_2, we used Dunnet's post test, using the BIF as the control treatment. In the western blotting and immunohistochemistry analyses, we used Bonferroni post test to compare all treatments. Statistical analysis of H^+-ATPase cellular staining was performed using the Kruskal–Wallis and Dunns' tests. In all cases, the fiducial level of significance was set at P<0.05.

Results

6 h infusions

Blood pH and plasma total CO_2

To control for potential effects of colchicine on basal acid/base regulatory processes, we monitored blood pH hourly in dogfish infused with NaCl for 3 h previous to and 6 h after the colchicine injection. As seen in Fig. 1, blood pH in the colchicine-treated, NaCl-infused fish (col-NaCl IF) remained between 7.8 and 7.9, while plasma TCO_2 ranged between 3.38 and 4.20 mmol l^{-1} (N=4). We did not find any significant differences in plasma osmolarity, [Na^+] or [Cl^-], nor did we notice any changes in fish activity.

Fig. 1A shows blood pH for the base-infused fish (BIF) and the colchicine-treated, base-infused fish (col-BIF). Both treatments induced a sharp increase in blood pH of ~0.25 pH units after 1 h of infusion, from ~7.90 to ~8.16 pH units. Although blood pH in the BIF had a tendency to drop by 6 h (8.07±0.07 pH units), it was not significantly lower than in the col-BIF (8.21±0.03 pH units) (N=4). During t=1–6 h, blood pH in both BI treatments was significantly higher than in the col-NaCl IF (7.82±0.05 pH units at t=6 h; P<0.05, N=4).

The TCO_2 graph (Fig. 1B) displayed a temporal pattern similar to that of blood pH: a rapid increase in both BIF and col-BIF followed by plateaus at values significantly higher than in the col-NaCl fish. However, unlike blood pH, TCO_2 in the col-BIF was significantly higher than in the BIF at t=4 and 6 h (11.31±1.41 *vs* 6.72±0.44 and 10.34±1.23 *vs* 6.42±0.33 mmol l^{-1}, respectively; P<0.05, N=4).

We did not find any significant differences in any other plasma variables at any of the times analyzed. Osmolarity ranged between 880 and 940 mosmol l^{-1}, [Na^+] was between 230 and 286 mmol l^{-1}, and [Cl^-] values were between 211 and 286 mmol l^{-1}.

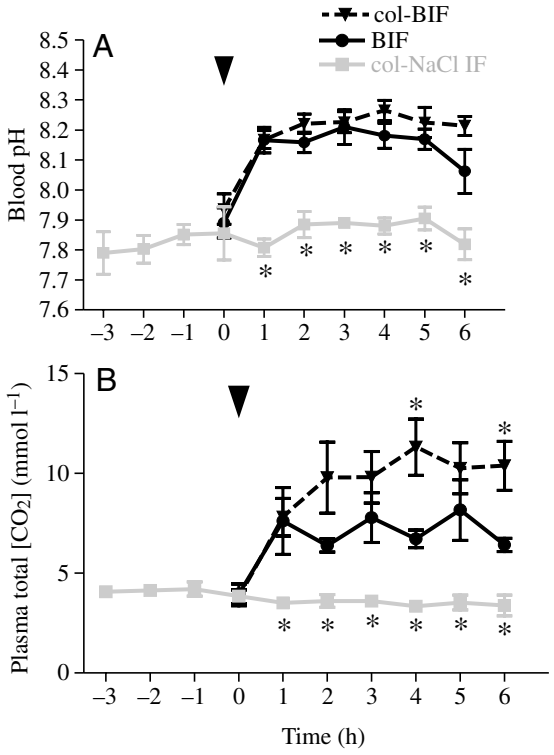

Fig. 1. 6 h infusions. Blood parameters of colchicine-treated NaCl-infused fish, HCO_3^--infused fish and colchicine-treated HCO_3^--infused fish (means ± s.e.m.). (A) Arterial blood pH. (B) Total CO_2 in plasma from arterial blood samples. The arrowheads indicate injection of colchicine (15 mg kg^{-1}). *P<0.05 compared with base-infused fish of the respective time (RM-ANOVA, 1-way ANOVA, Dunnet's post test) (N=4).

H^+-ATPase abundance

In agreement with our previous paper (Tresguerres et al., 2005), western analysis for H^+-ATPase revealed a distinct band of ~80 kDA. Fluorometric analysis on whole-gill

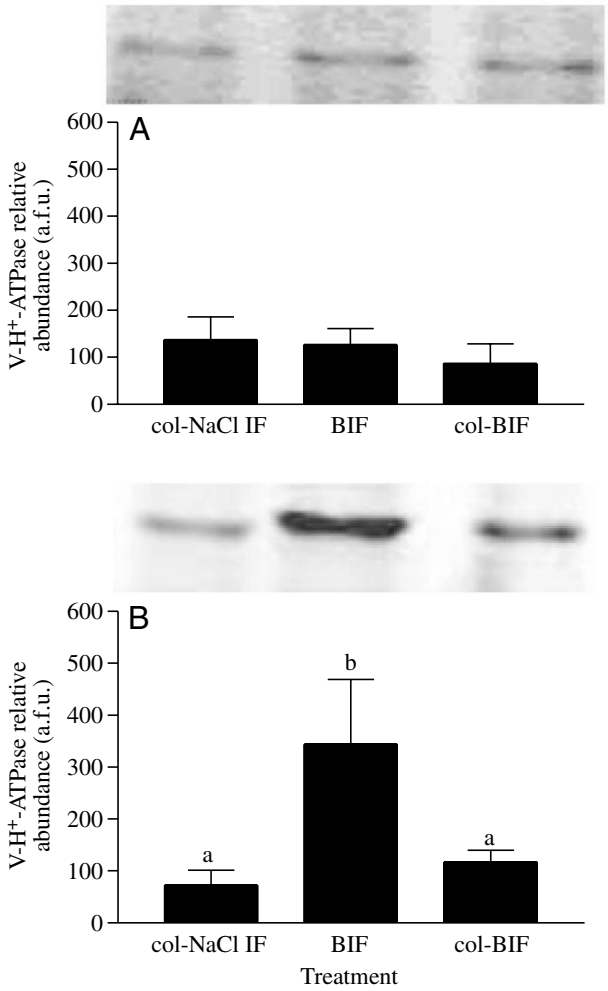

Fig. 2. 6 h infusions. Quantitative analysis of V-H^+-ATPase in gills from colchicine-treated, NaCl-infused (col-NaCl IF), base-infused (BIF) and colchicine-treated, base-infused (col-BIF) fish. (A) Whole-gill homogenates. (B) Membrane fraction. V-H^+-ATPase abundance was significantly greater only in the membrane fraction of BIF (N=4). Representative immunoblots are shown above each panel. The lower-case letters indicate difference levels of statistical significance (1-way ANOVA, Bonferroni's post test). Results are means ± s.e.m.

homogenates showed no significant differences in H$^+$-ATPase abundance between treatments (Fig. 2A). However, when the gill membrane fraction was assessed (Fig. 2B), we found a significant increase in H$^+$-ATPase abundance in the BIF (344±125 a.f.u.; P<0.05, N=4). The effect of the colchicine treatment on H$^+$-ATPase migration to the basolateral membrane is apparent at this stage in the col-BIF, since H$^+$-ATPase abundance in gill membranes from col-BIF and col-NaCl IF were not significantly different from each other (117±22 *vs* 72±29 a.f.u., respectively).

Number of H$^+$-ATPase-rich cells and cellular distribution

The number of H$^+$-ATPase-labelled cells in the gill epithelium of dogfish from the different treatments was estimated from low-power micrographs (Fig. 3A–C). The number of H$^+$-ATPase-rich cells per interlamellar space was 4.42±0.77 in the BIF, 4.32±0.92 in the col-BIF and 3.15±0.37 in the col-NaCl IF. However, the differences were not significant (Fig. 3D). Analysis of H$^+$-ATPase cellular distribution was performed using high-power micrographs (Fig. 4). The cellular distribution of H$^+$-ATPase was classified into one of three arbitrary patterns: (1) distinct cytoplasmic staining, (2) distinct basolateral staining and (3) a state intermediate between the former two. Examples of each of these patterns can be found in Fig. 4A–C. Most cells (86.03±7.72%) from col-NaCl IF had cytoplasmic H$^+$-ATPase staining, a percentage significantly higher than for both BIF and col-BIF. The intermediate staining pattern was found in 45% of the cells from col-BIF, 30% of cells from BIF and only ~9% of cells from col-NaCl IF. Almost 57% of the cells from BIF showed a distinct basolateral location, significantly higher than the ~24% found in the col-BIF and the scarce ~5% in the col-NaCl IF. Table 2 shows the mean percentages for the three groups, together with a detailed statistical analysis. These results are in agreement with the general trend for greater H$^+$-ATPase abundance found in gill membranes from BIF.

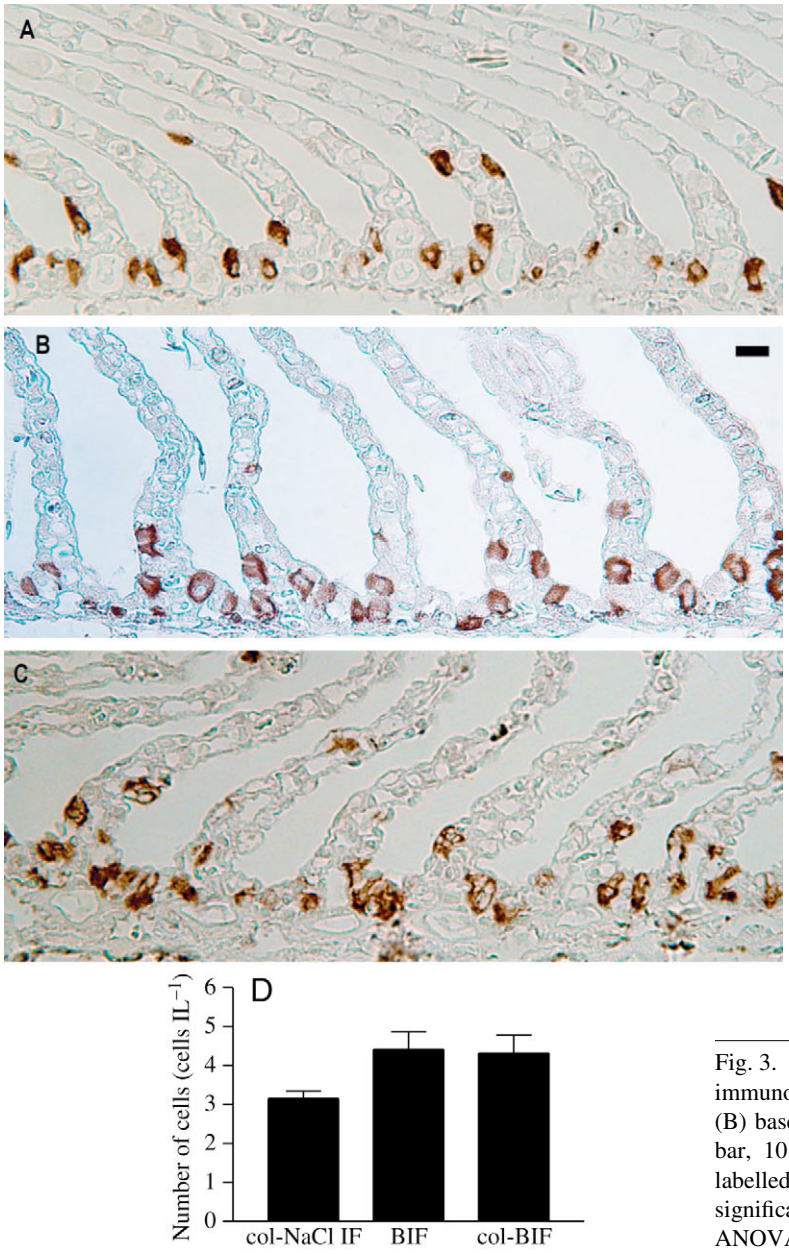

Fig. 3. 6 h infusions. Representative images of V-H$^+$-ATPase immunostaining in gills from (A) colchicine-treated, NaCl-infused, (B) base-infused and (C) colchicine-treated, base-infused fish. Scale bar, 10 μm. (D) The mean number of cells (± s.e.m.; N=4) that labelled for H$^+$-ATPase per interlamellar space (cells IL^{-1}). No significant differences were found between treatments (1-way ANOVA, Bonferroni's post test).

24 h infusions

Blood pH and plasma total CO_2

Fig. 5A shows blood pH in the 24 h-infusion experiments. In the first 6 h of the 24 h infusions, blood pH in all the treatments behaved identically to the 6 h infusions explained above. Even by t=9 h, pH in the col-BIF was higher than in the BIF, although not statistically significant. However, from t=12 h onward, blood pH from the col-BIF was found to be significantly more alkalotic than in the BIF, an effect that was greatest at t=24 h (8.33±0.06 *vs* 8.02±0.03 pH units; P=<0.05, N=5). Blood pH in the col-NaCl IF was relatively stable throughout the infusions, with values between 7.78±0.02 and 7.91±0.03 pH units. These values were significantly lower than the BIF and col-BIF from t=1 until the end of the experiments (P<0.05, N=5).

In this experimental series, TCO_2 from col-BIF was significantly higher than in BIF at 3 h (11.80 ±1.99 *vs* 6.90±0.93 mmol l^{-1}; P<0.05, N=5), and 6 h (13.12±3.10 *vs* 5.60±0.84 mmol l^{-1}; P<0.05,

N=5). While the difference in TCO_2 between col-BIF and BIF was reduced at *t*=9 and 12 h, it became statistically significant again at *t*=18 and 24 h ($P<0.05$, *N*=5). At 24 h, TCO_2 in the col-BIF was 15.72±3.29 mmol l^{-1}, compared with 6.74±1.34 mmol l^{-1} in the BIF. Col-NaCl IF had lower and very stable TCO_2 values, which ranged between 3.52±0.40 and 4.16±0.39 mmol l^{-1}. Importantly, TCO_2 from BIF and col-NaCl IF did not differ significantly at 24 h (Fig. 5B). Plasma osmolarity, $[Na^+]$ and $[Cl^-]$ remained stable for the experimentation period (not shown).

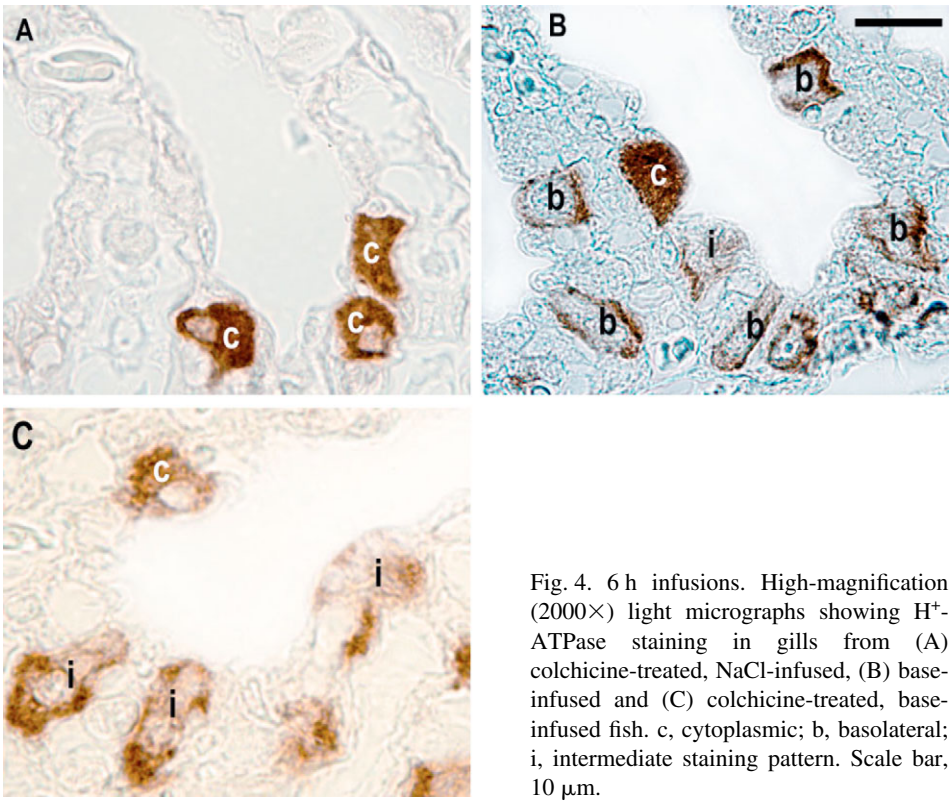

Fig. 4. 6 h infusions. High-magnification (2000×) light micrographs showing H^+-ATPase staining in gills from (A) colchicine-treated, NaCl-infused, (B) base-infused and (C) colchicine-treated, base-infused fish. c, cytoplasmic; b, basolateral; i, intermediate staining pattern. Scale bar, 10 μm.

H^+-ATPase abundance

H^+-ATPase from BIF gill samples was more abundant than in col-NaCl IF, both in whole-gill homogenates (198.4±38.9 *vs* 68.5±17.0 a.f.u.) and in the gill membrane-enriched fraction (574.6±168.1 *vs* 49.0±10.6 a.f.u.). This suggests an additional response (i.e. protein synthesis) to the H^+-ATPase translocation to the basolateral membrane observed in BIF from the 6 h-infusion experiments. Whole-gill samples from col-BIF showed a response that was intermediate between BIF and col-NaCl IF. Similar to the 6 h infusions, colchicine prevented the movement of H^+-ATPase to the basolateral membrane in the col-BIF, since H^+-ATPase abundance in the gill membrane fraction was not significantly different from in the col-NaCl IF (155.5±51.3 *vs* 49.0±10.6 a.f.u., respectively) (Fig. 6).

Number of H^+-ATPase-rich cells and cellular distribution

Fig. 7 shows representative images of gill sections from the three experimental groups. While we found a tendency for roughly one more H^+-ATPase-immunoreactive cell per interlamellar space in the BIF and col-BIF compared with the col-NaCl IF (5.01±0.73, 4.97±0.32 and 3.75±0.82 cells IL^{-1}, respectively; Fig. 7D), the difference was not significant.

The cellular H^+-ATPase staining pattern was fairly homogeneous in the col-NaCl IF, where over 91% of the cells had cytoplasmic staining, and in the BIF, with 84% of cells showing a distinctly basolateral staining pattern. The staining pattern in the col-BIF was unique, with an in-between percentage of cells with cytoplasmic and basolateral staining patterns but with more cells displaying the intermediate pattern (~44% of cells *vs* ~10% in both the BIF and col-NaCl IF). Representative pictures and a summary of the staining patterns are shown in Fig. 8 and Table 3, respectively.

Table 2. *6 h infusions. H^+-ATPase staining patterns in gills from colchicine-treated, NaCl-infused (col-NaCl IF), base-infused (BIF) and colchicine-treated, base-infused fish (col-BIF)*

	Cells (*n*)	Cytoplasmic (%)	Intermediate (%)	Basolateral (%)
Col-NaCl	202	86.03±7.72[a]	8.62±5.26[a]	5.36±3.42[a]
BIF	241	13.42±5.13[b]	29.63±11.07[a,b]	56.95±13.42[b]
Col-BIF	208	31.47±5.51[b]	44.90±5.42[b]	23.63±6.30[a]

Lower-case letters indicate different levels of statistical significance within each column (Kruskal-Wallis test, Dunns' post test). Results are means ± s.e.m.

Discussion

Microtubule-dependent translocation of H^+-ATPase from the cytoplasm to the cell membrane has been demonstrated for a variety of mammalian ion-transporting epithelia, most notably the kidney (reviewed by Wagner et al., 2004). In particular, microtubules have been shown to mediate the translocation of H^+-ATPase to the apical membrane of renal tubule intercalated cells (IC) in response to a variety of stimuli, including acid incubation (Schwartz et al., 2002), angiotensin II (Wagner et al., 1998) and aldosterone (Winter et al., 2003). Microtubules also determine the constitutive apical and basolateral localization of H^+-ATPase in the acid-secreting (A-type) and in the base-secreting (B-type) IC, respectively (Brown et al., 1991). Contrary to the mammalian kidney,

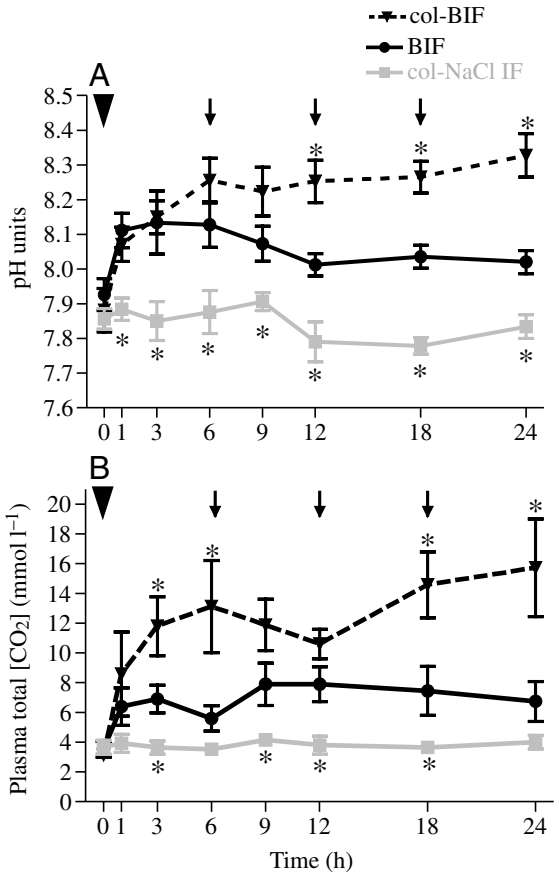

Fig. 5. 24 h infusions. Blood parameters of colchicine-treated NaCl-infused fish (col-NaCl IF), $NaHCO_3$-infused fish (BIF), and colchicine-treated $NaHCO_3$-infused fish (col-BIF) (means ± s.e.m.). (A) Arterial blood pH. (B) Total CO_2 in plasma from arterial blood samples. The arrowheads indicate a bolus injection of colchicine (15 mg kg^{-1}). Subsequent arrows indicate injection of half doses of colchicine (7.5 mg kg^{-1}). *P<0.05 compared with base-infused fish of the respective time (RM-ANOVA, 1-way ANOVA, Dunnet's post test) (N=5).

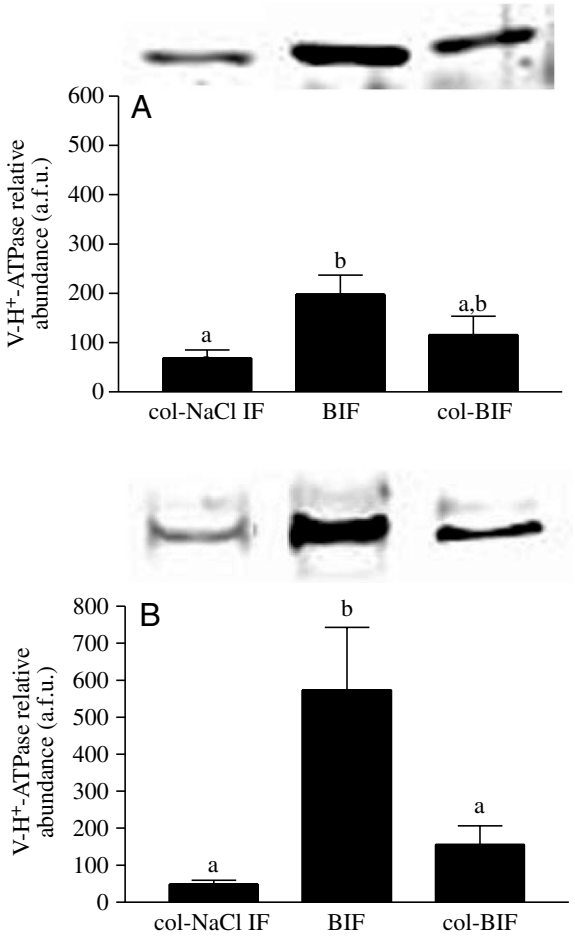

Fig. 6. 24 h infusions. Quantitative analysis of V-H^+-ATPase in gills from colchicine-treated, NaCl-infused (col-NaCl IF; N=4), base-infused (BIF; N=5) and colchicine-treated, base-infused fish (col-BIF; N=5). (A) Whole-gill homogenates. (B) Membrane fraction. Representative immunoblots are shown above each panel. The lower-case letters indicate difference levels of statistical significance (1-way ANOVA, Bonferroni's post test). Results are means ± s.e.m.

information about ion-transporting processes that rely on an intact cytoskeleton to mediate H^+-ATPase relocalization is much scarcer in other animal taxonomic groups. Some exceptions include urinary acidification in the turtle bladder (Gluck et al., 1982) and ammonia excretion across crustacean gills (Weihrauch et al., 2002). We could not find any references specifically linking H^+-ATPase translocation to microtubules in any group of fishes (teleosts, elasmobranches, etc.). However, the use of colchicine in fish transport physiology includes salt secretion in the seawater-adapted grey mullet, *Mugil capito* (Maetz and Pic, 1976), urea excretion in the Gulf toadfish, *Opsanus beta* (Gilmour et al., 1998), and calcium uptake in larvae of tilapia, *Oreochromis mossambicus* (Tsai and Hwang, 1998).

Our results suggest that upregulation of branchial base secretion in the dogfish depends on the microtubule-dependent translocation of H^+-ATPase to the basolateral membrane. When this process is prevented by colchicine, it correlates with increased blood pH and TCO_2, indicating an impaired capacity to secrete excess base. The sections immunostained against H^+-ATPase confirmed the inhibitory effect of colchicine on H^+-ATPase translocation to the basolateral membrane. Originally, we intended to classify the staining patterns into either cytoplasmic or basolateral. Although most of the cells from the col-NaCl IF fit into the first category and the majority of cells from BIF fit into the second category, some cells displayed an intermediate staining pattern and were classified into a third category. We believe that this nicely illustrates the dynamic aspects of the H^+-ATPase translocation process, whereby there is a continuum of staining patterns between cytoplasmic and distinctly basolateral.

If the effect of the colchicine was completely effective, we would expect a predominant cytoplasmic staining in the col-BIF. However, we found that the intermediate pattern showed the highest frequency. Also, based on our infusion rates, we might predict higher elevations in pH and TCO_2 if base

Table 3. *24 h infusions. H^+-ATPase staining patterns in gills from colchicine-treated, NaCl-infused (col-NaCl IF), base-infused (BIF) and colchicine-treated, base-infused fish (col-BIF)*

	Cells (n)	Cytoplasmic (%)	Intermediate (%)	Basolateral (%)
Col-NaCl	212	90.9±4.49[a]	9.72±5.09[a]	3.33±3.33[a]
BIF	393	4.94±1.06[b]	10.83±1.54[a]	84.22±2.29[b]
Col-BIF	324	32.50±4.03[c]	43.69±6.92[b]	23.82±4.97[c]

Lower-case letters indicate different levels of statistical significance within each column (Kruskal-Wallis test, Dunns' post test). Results are means ± s.e.m.

secretion was totally impaired. Taken together, these data suggest that colchicine only had a partial effect on blocking the H^+-ATPase translocation to the basolateral membrane. Interestingly, microtubule-disrupting drugs only inhibit between 50 and 70% of acid and base secretion by A-type and B-type ICs (Brown and Stow, 1996). These authors suggested that random vesicle movement resulted in fusion of H^+-ATPase-containing vesicles to the appropriate target membrane.

Western blotting and immunohistochemistry analyses indicate that the base secretory mechanism that allows BIF to regulate blood pH and TCO_2 despite continuous infusion of HCO_3^-, includes two components. In the short term (6 h), the pool of H^+-ATPase already present in cytoplasmic vesicles moves to the basolateral membrane in a microtubule-dependent manner. In the longer term (24 h), there is an addition upregulation in the synthesis of H^+-ATPase, as demonstrated by increased abundance in the whole-gill homogenates. Since the number of H^+-ATPase-rich cells per interlamellar space did not differ between treatments, we suggest that this increase takes place in already existing H^+-ATPase-rich cells rather than being due to the appearance of new base-secreting cells. However, the samples used for H^+-ATPase-rich cell enumeration were only from the trailing edge of gill filaments. We cannot discount the possibility that the number of H^+-ATPase-rich cells in other parts of the filament increases after 24 h of infusion, which could be contributing to the sharp increase in H^+-ATPase abundance found in 24 h BIF.

The presence of specialized base-secreting cells in the gill epithelium of marine elasmobranches is well supported by this and other studies. Gill H^+-ATPase-rich cells possess the apical anion exchanger Pendrin (Piermarini et al., 2002; Evans et al., 2004) and cytoplasmic H^+-ATPase-containing vesicles (Wilson et al., 1997; Piermarini and Evans, 2001; Piermarini et al., 2002; Choe et al., 2005; Tresguerres et al., 2005). When blood gets alkalotic, H^+-ATPase inserts to the basolateral membrane in a microtubule-dependent manner to mediate base secretion, thus contributing to restoring blood pH to normal values. In this configuration, the H^+-ATPase-rich cells closely resemble the B-type IC from the

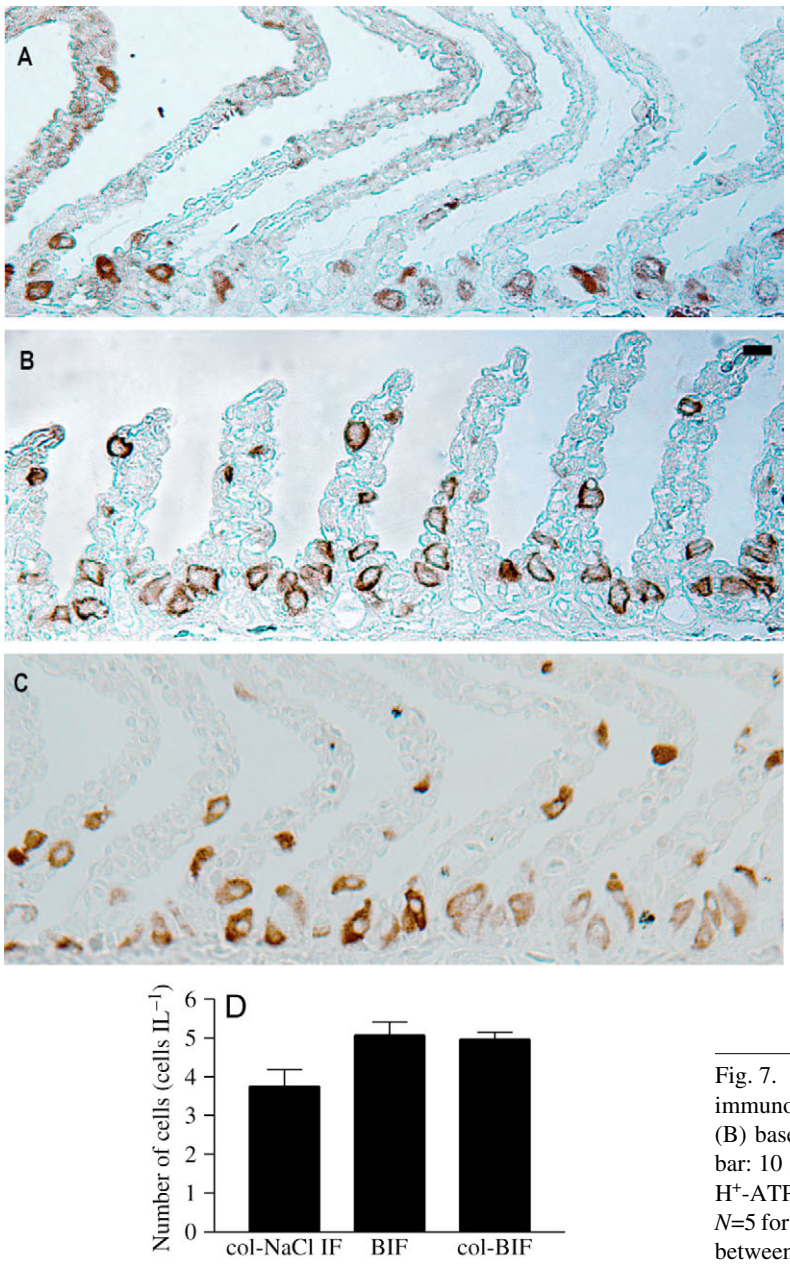

Fig. 7. 24 h infusions. Representative images of V-H^+-ATPase immunostaining in gills from (A) colchicine-treated, NaCl-infused, (B) base-infused and (C) colchicine-treated, base-infused fish. Scale bar: 10 μm. (D) The mean number of cells (± s.e.m.) that labelled for H^+-ATPase per interlamellar space (cells IL^{-1}) (N=4 for col-NaCl IF, N=5 for the other two groups). No significant differences were found between treatments (1-way ANOVA, Bonferroni's post test).

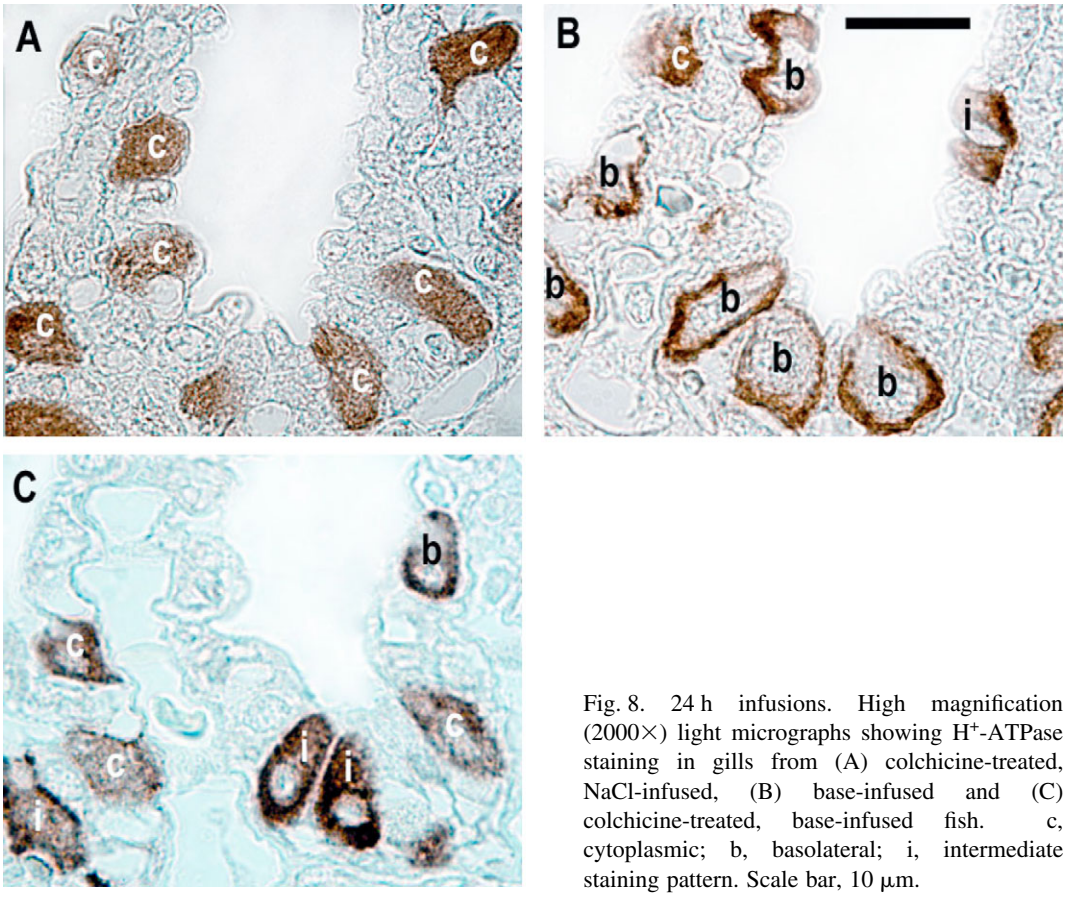

Fig. 8. 24 h infusions. High magnification (2000×) light micrographs showing H^+-ATPase staining in gills from (A) colchicine-treated, NaCl-infused, (B) base-infused and (C) colchicine-treated, base-infused fish. c, cytoplasmic; b, basolateral; i, intermediate staining pattern. Scale bar, 10 μm.

mammalian kidney. Continuous alkalotic stress induces an upregulation in the synthesis of H^+-ATPase units. The model for the H^+-ATPase-rich cell also includes cytoplasmic carbonic anhydrase (CA) to catalyze the conversion of CO_2 into HCO_3^- and H^+, the substrates for H^+-ATPase and Pendrin, respectively. The involvement of CA in branchial base secretion has been documented as early as 1955 (Hodler et al., 1955) and was confirmed by later studies (e.g. Swenson and Maren, 1987). Furthermore, CA II-like immunoreactiviy has been detected in mitochondria-rich (MR) cells of the dogfish gill epithelium (Wilson et al., 2000), although it has not been demonstrated if CA colocalizes with H^+-ATPase and/or Pendrin in the same type of MR cells. We predict that H^+-ATPase-rich cells should also have a chloride channel in the basolateral membrane to move Cl^- that enters the cell through the apical membrane into the blood. This Cl^- current would be essential to compensate for the inside-negative transmembrane potential generated by the H^+-ATPase (cf. Wagner et al., 2004). A model for base secretion in H^+-ATPase-rich cells is illustrated in Fig. 9.

The correlation between H^+-ATPase localization and recovery from the alkalotic stress found in the current study is very strong. However, we must also consider that colchicine might also affect other cellular components that might act directly or indirectly on the base-secreting properties of the animal. An example of a possible direct effect would be that microtubule disruption affects the trafficking of the apical anion exchanger. Alternatively, our results may be explained by a non-target effect on a cell type elsewhere in the body whereby colchicine affects hormone release, which in turn alters the mechanism of base secretion. Unfortunately, nothing is known about the hormonal pathways involved in acid/base regulation in fish, so we are unable to either control for or discuss this topic further. Nonetheless, it must be kept in mind that factors other than microtubule-dependent H^+-ATPase redistribution might be responsible for the reduced ability to recover from an alkalotic load. However, our results demonstrate that microtubule-dependent translocation of H^+-ATPase from the cytoplasm to the cell membrane is associated with enhanced secretion of HCO_3^- across the gills of the dogfish.

In summary, our results strongly suggest that blood alkalosis induces the translocation of gill H^+-ATPase from cytoplasmic vesicles to the basolateral membrane in a microtubule-dependent manner. Based on the effect of colchicine on blood pH and plasma TCO_2 from base-infused fish, and on the predominant role that the gills have on dogfish base secretion over other organs (Hodler et al., 1955; Heisler, 1988), we propose that this process is essential for branchial transepithelial base secretion and maintenance of blood pH within homeostatic limits.

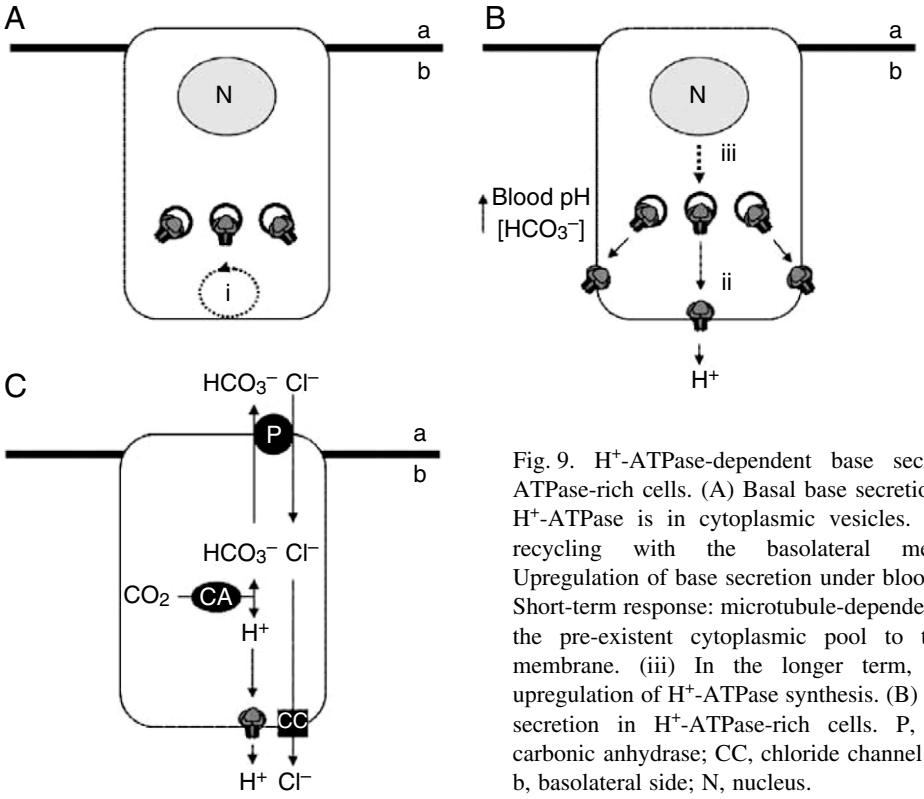

Fig. 9. H^+-ATPase-dependent base secretion in H^+-ATPase-rich cells. (A) Basal base secretion. Most of the H^+-ATPase is in cytoplasmic vesicles. (i) Continuous recycling with the basolateral membrane. (B) Upregulation of base secretion under blood alkalosis. (ii) Short-term response: microtubule-dependent relocation of the pre-existent cytoplasmic pool to the basolateral membrane. (iii) In the longer term, there is also upregulation of H^+-ATPase synthesis. (B) Model for base secretion in H^+-ATPase-rich cells. P, Pendrin; CA, carbonic anhydrase; CC, chloride channel; a, apical side; b, basolateral side; N, nucleus.

This research was funded by an NSERC Discovery grant (G.G.G.), the Donald Ross Scholarship and the Izaak Walton Killam Memorial Scholarship (M.T.) and an Alberta Ingenuity post-doctoral fellowship (F.K.). We would like to acknowledge the invaluable help by the Bamfield Marine Centre research co-ordinator, Dr Bruce A. Cameron. We are also indebted to Dr Colin Brauner's lab for insightful discussion of data and use of equipment, and to Dan Baker in particular for, in addition, measuring total CO_2 in the plasma samples from the 24 h experiments.

References

Brown, D. (2000). Targeting of membrane transporters in renal epithelia: when cell biology meets physiology. *Am. J. Physiol. Renal Physiol.* **278**, F192-F201.

Brown, D. and Stow, J. I. (1996). Protein trafficking and polarity in kidney epithelium: from cell biology to physiology. *Physiol. Rev.* **76**, 245-297.

Brown, D. I., Sabolic, I. and Gluck, S. (1991). Colchicine-induced redistribution of proton pumps in the proximal tubule. *Kidney Int.* **40**, S79-S83.

Choe, K. P., Kato, A., Hirose, S., Plata, C., Sindic, A., Romero, M. F., Claiborne, J. B. and Evans, D. H. (2005). NHE3 in an ancestral vertebrate: primary sequence, distribution, localization, and function in gills. *Am. J. Physiol.* **289**, R1520-R1534.

Evans, D. H., Piermarini, P. M. and Choe, K. P. (2004). Homeostasis: osmoregulation, pH regulation, and nitrogen excretion. In *Biology of Sharks and their Relatives* (ed. J. C. Carrier, J. A. Musick and M. R. Heithaus), pp. 247-268. Boca Raton, FL: CRC Press.

Evans, D. H., Piermarini, P. M. and Choe, K. P. (2005). The multifunctional fish gill: dominant site of gas exchange, osmoregulation, acid-base regulation, and excretion of nitrogenous waste. *Physiol. Rev.* **85**, 97-177.

Gilmour, K. M., Perry, S. F., Wood, C. M., Henry, R. P., Laurent, P., Part, P. and Walsh, P. J. (1998). Nitrogen excretion and the cardiorespiratory physiology of the gulf toadfish, *Opsanus beta*. *Physiol. Zool.* **71**, 492-505.

Gluck, S., Cannon, C. and Al-Awqati, Q. (1982). Exocytosis regulates urinary acidification in turtle bladder by rapid insertion of H^+ pumps into the luminal membrane. *Proc. Natl. Acad. Sci. USA* **79**, 4327-4331.

Heisler, N. (1988). Acid-base regulation. In *Physiology of Elasmobranch Fishes* (ed. T. J. Shuttleworth), pp. 215-252. Berlin: Springer-Verlag.

Hodler, J., Heinemann, H. O., Fishman, A. P. and Smith, H. W. (1955). Urine pH and carbonic anhydrase activity in the marine dogfish. *Am. J. Physiol.* **183**, 155-162.

Humason, G. L. (1962). Hematoxylin staining. In *Animal Tissue Techniques* (ed. R. Emerson, D. Kennedy, R. B. Park, G. W. Beadle and D. M. Witaker), pp. 136-154. San Francisco, London: W. H. Freeman and Co.

Katoh, F., Hyodo, S. and Kaneko, T. (2003). Vacuolar-type proton pump in the basolateral plasma membrane energizes ion uptake in branchial mitochondria-rich cells of killifish Fundulus heteroclitus, adapted to a low ion environment. *J. Exp. Biol.* **206**, 793-803.

Laemmli, U. K. (1970). Cleavage of structural proteins during the assembly of the head of the bacteriophage T4. *Nature* **227**, 680-685.

Maetz, J. and Pic, P. (1976). Microtubules in the 'chloride cell' of the gill and disruptive effects of colchicine on the salt balance of the seawater-adapted *Mugil capito*. *J. Exp. Zool.* **199**, 325-338.

Moffat, A. C. (1986). In *Clarke's Isolation and Identification of Drugs*, second edition (ed. C. A. Moffat, J. V. Jackson, M. S. Moss and B. Widdop), p. 492. London: The Pharmaceutical Press.

Piermarini, P. M. and Evans, D. H. (2001). Immunochemical analysis of the vacuolar proton-ATPase B-subunit in the gills of a euryhaline stingray (*Dasyatis sabina*): effects of salinity and relation to Na^+/K^+-ATPase. *J. Exp. Biol.* **204**, 3251-3259.

Piermarini, P. M., Verlander, J. W., Royaux, I. E. and Evans, D. H. (2002). Pendrin immunoreactivity in the gill epithelium of a euryhaline elasmobranch. *Am. J. Physiol.* **283**, R983-R992.

Schwartz, G. J., Tsuruoka, S., Vijayakumar, S., Petrovic, S., Mian, A. and Al-Awaqati, Q. (2002). Acid incubation reverses the polarity of intercalated cell transporters, an effect mediated by hensin. *J. Clin. Invest.* **109**, 89-99.

Stephens, R. E. and Edds, K. T. (1976). Microtubules: structure, chemistry, and function. *Physiol. Rev.* **56**, 709-777.

Swenson, E. R. and Maren, T. H. (1987). Roles of gill and red cell carbonic

anhydrase in elasmobranch HCO_3- and CO_2 excretion. *Am. J. Physiol.* **253**, R450-R458.

Tresguerres, M., Katoh, F., Fenton, H., Jasinska, E. and Goss, G. G. (2005). Regulation of branchial V-H^+-ATPase, Na^+/K^+-ATPase and NHE2 in response to acid and base infusions in the Pacific spiny dogfish (*Squalus acanthias*). *J. Exp. Biol.* **208**, 345-354.

Tsai, J. C. and Hwang, P. P. (1998). Effects of wheat germ agglutinin and colchicine on microtubules of the mitochondria-rich cells and Ca^{2+} uptake in tilapia (*Oreochromis mossambicus*) larvae. *J. Exp. Biol.* **201**, 2263-2272.

Wagner, C. A., Giebisch, G., Lang, F. and Geibel, J. P. (1998). Angiotensin II stimulates vesicular H^+-ATPase in rat proximal tubular cells. *Proc. Natl. Acad. Sci. USA* **95**, 9665-9668.

Wagner, C. A., Finberg, K. E., Breton, S., Marshansky, V., Brown, D. and Geibel, J. P. (2004). Renal vacuolar H^+-ATPase. *Physiol. Rev.* **84**, 1263-1314.

Weihrauch, D., Ziegler, A., Siebers, D. and Towle, D. W. (2002). Active ammonia excretion across the gills of the green shore crab *Carcinus maenas*: participation of Na^+/K^+-ATPase, V-type H^+-ATPase and functional microtubules. *J. Exp. Biol.* **205**, 2765-2775.

Wilson, J. M., Randall, D. J., Vogl, A. W. and Iwama, G. K. (1997). Immunolocalization of proton-ATPase in the gills of the elasmobranch, *Squalus acanthias*. *J. Exp. Zool.* **278**, 78-86.

Wilson, J. M., Randall, D. J., Vogl, A. W., Harris, J., Sly, W. S. and Iwama, G. K. (2000). Branchial carbonic anhydrase is present in the dogfish, *Squalus acanthias*. *Fish Physiol. Biochem.* **22**, 329-336.

Winter, C., Schulz, N., Giebisch, G., Geibel, J. P. and Wagner, C. A. (2004). Nongenomic stimulation of vacuolar H^+-ATPase in intercalated renal tubule cells by aldosterone. *Proc. Natl. Acad. Sci. USA* **101**, 2636-2641.

Zall, D. M., Fischer, M. D. and Garner, Q. M. (1956). Photometric determination of chloride in water. *Anal. Chem.* **28**, 1665-1678.